

DESIGN METHODOLOGY FOR BRIDGE ABUTMENT PILE GROUP FOUNDATIONS – A CASE STUDY

A.V. Batilas*, B. Bahmani, D.P. Bannister, D.M. Roberts and A.D. Benson

Atkins (Member of SNC Lavalin), Birmingham, UK

* Corresponding author

ABSTRACT A reliable assessment of immediate and long-term deflections is vital for a cost-effective pile group design supporting a bridge abutment. This paper reports on some key challenges involved in the design methodology developed for the assessment of 8 over bridges on a railway scheme in UK. The unconventional construction sequence involved placement and locking of the bridge deck prior to backfilling. This resulted in reduction of the allowable translational and rotational movements of the abutments' foundations to eliminate the risk of exceeding the bearings' movement tolerances. To test this scenario and based on engineering judgement, careful interpretation of the available field, laboratory and numerical analysis results was carried out, and the use of at-rest (K_0) static earth pressure is considered to be suitable in pile design for the case where the foundations are required to be comparatively rigid to meet the above performance criteria. Also, as part of the design process, the output of linear and non-linear analysis from commonly used pile group analysis software packages: Repute and PIGLET were compared with finite element analysis using Plaxis 3D which are presented.

1. Introduction

Movement of bridge abutments is significantly important when considering the overall serviceability and safety of the structure. A reliable assessment of the lateral earth pressure distribution and the immediate and long-term deflections is vital in order to create a cost-effective design which satisfies the design requirements.

Earth pressure distribution behind retaining wall systems is a soil-structure interaction problem and therefore should be determined interactively with the deflection of the wall. In the current design practice, the earth pressure distribution behind the wall is adopted according to the at-rest or active earth pressure theories. However, relatively 'non-yielding walls' such as bridge abutments on stiff piles usually undergo relatively small movement which can be insufficient to initiate the sliding wedge behind the wall and to relieve the pressure to its active or passive state (El-Emam, 2011).

In this study, each bridge comprised inverted 'nonyielding' T-shape abutments and wingwalls founded on two rows of circular concrete piles with an off-centre abutment stem creating a longer heel. The bridge deck is supported on elastomeric bearings on both sides. Anticipated deflections in the bearings were of concern due to (a) an unconventional construction sequence which involved placement and locking of the deck prior to backfilling substructure to streamline the scheme's construction sequence and (b) high estimated lateral loading induced by traffic and backfill material. As a result of the above construction sequence and the required structure rigidity, the anticipated movement of the structure was thought to be unlikely to be enough to mobilise the active state. In order to make an informed decision about the mobilisation of active (K_a) or at-rest (K_0) static earth pressure, analytical and numerical analysis was conducted and the results were interpreted against field and laboratory data as well as published literature.

It is important to note that this paper follows the design methodology developed for the design of the substructures of a major railway scheme in the UK. More specifically, the

- details about the typical geometry of the bridge,
- geotechnical investigation and the advanced in-situ and laboratory testing which are required to consider the soil non-linearity in routine design, and
- unconventional construction stages are presented.

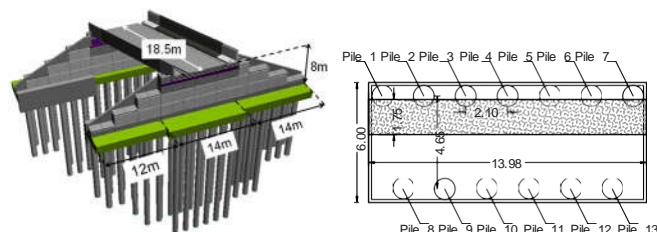
As part of the development of the design methodology it was observed that despite availability of many different pile group design software packages, little information could be found to compare the results of analyses carried out with alternative programs (Pirrello and Poulos, 2013). Therefore, a comparison is made between the results obtained from Repute and PIGLET which are often used in current pile design practice against PLAXIS 3D.

2. Description of Typical Structure

2.1 Structure geometry

For the purpose of this paper, a representative structure was selected. The proposed structure is a semi-integral bridge with a clear square span of 18.5m. The substructure comprised abutment walls and parallel wingwalls built from precast concrete units. The substructure is supported by individual pile caps which function individually (Figure 1). The abutment retained height from the top of the pile cap to the top of the road level is ~8.7m and the abutment length is ~14m long which is supported on a pile cap 1.5m thick by 6m wide.

Figure 1 Three-dimensional view of structure including sub structure and abutment pile cap arrangement.



2.2 Construction sequence

The construction sequence of the bridge is as follows:

1. Installation of piles and pile caps
2. Construction of the abutments and wingwalls
3. Installation of bearings followed by bridge deck locking
4. Placing and compaction of the backfill

2.3 Foundation Details

The substructure is supported by a 1.5m thick pile cap connecting 1050mm diameter bored concrete piles with a total embedment length of 23m. The base of the pile cap is +88mAOD. As shown in Figure 1, the piles are arranged in a staggered formation with spacings of 2.1m and 4.65m in the x and y axis respectively.

3. Description of Geology and Subsurface Conditions

3.1 Regional & local geology and soil features

The local ground conditions consist of minor thicknesses of cohesive glacial deposits (CGD) in the form of firm to stiff clay to a depth of 1.3mbgl. These deposits overlie the Oxford Clay Formation (Peterborough member) which encompasses a 4m weathered zone characterised as firm to locally stiff clay (OXC-PET (W)) overlying unweathered Oxford Clay (OXC-PET (UW)) characterised as stiff to very stiff clay (tending to extremely weak Mudstone) as shown in Figure 2.

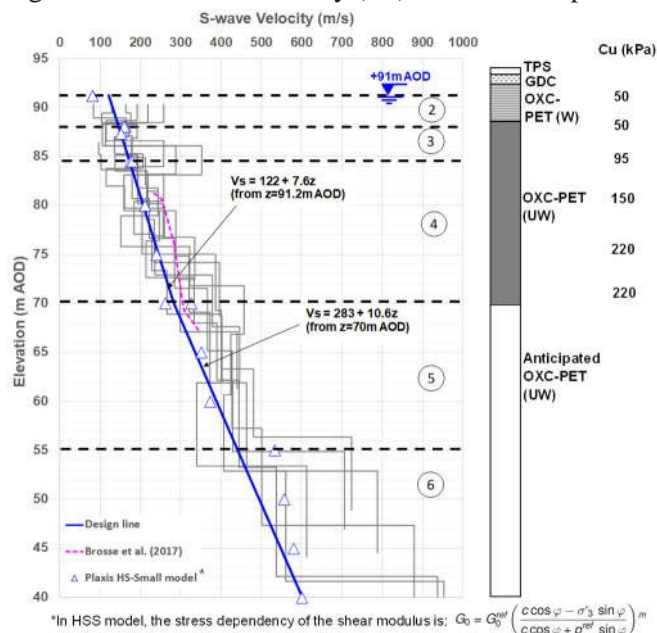
3.2 Geotechnical investigation

The subsurface investigation of the examined area consists of a combination of a) borings with sampling and SPT measurements to a depth of 20m, b) hand shear vane tests in trial pits and c) in-situ evaluation of low-strain shear wave velocity, V_s , at 3 locations within 100m by Surface Wave Methods: Multi-channel Analysis of Surface Waves (MASW) and Refraction Microtremor (ReMi). Self-boring pressuremeter testing (SBPM) was made available at a site ~15km away conducted in Mid and Lower OXC Formation with similar ground conditions. Figure 2 shows the V_s -depth profile which agreed well with results obtained from literature (Brosse et al., 2017). Laboratory testing consisted predominantly of measurement of limited number of advanced K_0 -consolidated undrained triaxial with local strain gauges (CK₀U) as well as oedometer testing. Similar lab and field testing from the wider site were also available and used in conjunction with the site-specific data.

3.3 Pile load test result

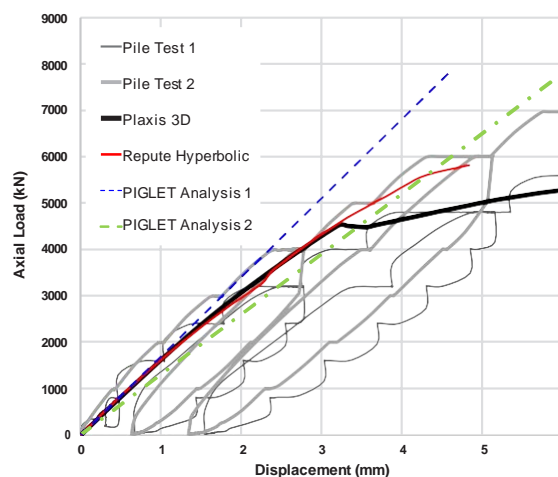
Although pile load tests are very useful in developing an efficient design, no preliminary pile testing was conducted in the examined area. However, the results of two pile load tests undertaken on 0.9m dia test piles 25m in length were available from other locations in the UK with similar ground conditions (Vardanega et al., 2019). The pile group analyses conducted as part of the design (see Section 5.2) included both linear and non-linear load-displacement behaviour of the

Figure 2 Shear wave velocity (V_s) vs. elevation profile



pile groups. To make an informed decision about the parameters to be used in the pile group analysis software (see section 5.2) and on the basis of engineering judgement, the load-settlement behaviour of a single pile was modelled in Repute, Plaxis 3D and PIGLET against the aforementioned pile load test data as shown in Figure 3.

Figure 3 Vertical load-settlement behaviour compared to the pile load test results



4. Design Methodology

4.1 Bridge load combination

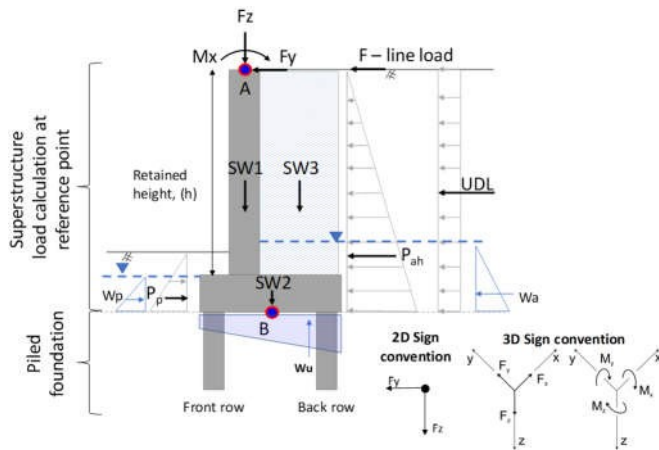
The forces and moments acting on the structure have been calculated and resolved about the centre of the pile cap (point B) as illustrated in Figure 4. The resultant forces and moments have been calculated from the following:

- a) Structural loading at the deck bearing level including the structures self-weight (F, M at point A);

- b) Traffic loading in accordance with PD6694-1:2011 section 7 (F line load, UDL);
- c) Active (P_{ah}) and passive (P_p) earth pressures;
- d) Permanent self-weight (SW); and
- e) Hydrostatic pressures (w).

The load combinations used in the pile group analyses are given in Table 1.

Figure 4 Load combination diagram



4.2 Pile group analysis software

Methods employed by commercial software packages for the design of pile groups are predominantly the Boundary Element Analysis (BEM) and the Finite Element Method (FEM). In this study, PIGLET, Repute and Plaxis 3D are used as tools to employ the analysis methods. The basis and limitations of each software are described by Pirello and Poulos (2013).

Table 1 Load combinations used in pile group analyses

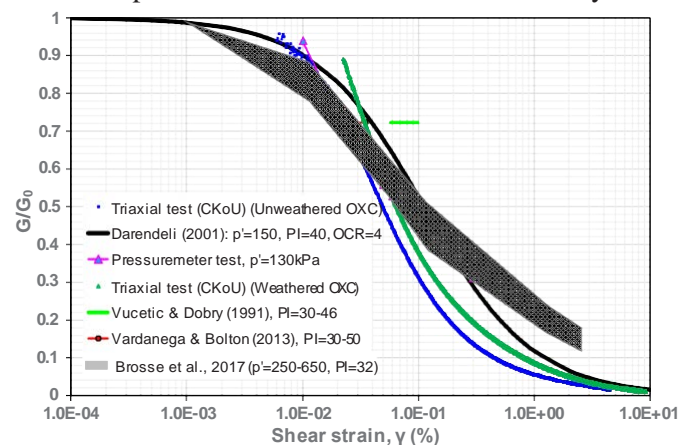
Load case	Fx (kN)	Fy (kN)	Fz (kN)	Mx (kNm)	My (kNm)	Mz (kNm)
2D Analysis Structural Loading Input (at point A: bearing level)						
Permanent	6	16	282	0	-62	0
Variable	9	-7	68	0	-69	-34
3D Analysis Geotechnical and Structural Loading Input (at point B: bottom of pile cap)						
Permanent	83	5126	17565	-18470	-144	105
Variable	388	836	953	-6078	3466	631

Note: Fx is into the page

4.3 Soil model input parameters

The very small strain ($\sim 10^{-4}$ %) shear modulus (G_0) parameter in this study is derived from surface wave measurements (Figure 2). Unlike the small strain stiffness, the knowledge of $\gamma_{0.7}$ first requires the measurement of G_0 (e.g. geophysical survey, bender element testing) followed by the measurement of shear modulus at small ($\sim 10^{-2}$ %) to large strain level (e.g. advanced triaxial with local gauges triaxial, resonant column and pressuremeter test). Next, the normalised stiffness degradation curve can be constructed and the $\gamma_{0.7}$ can be read from the curve (Figure 5). $\gamma_{0.7}$ is later utilised in the Hardening Soil Small (HSS) model in Plaxis. The reference threshold shear strain ($\gamma_{0.7}$) is regarded herewith as a soil parameter to

Figure 5 Comparison of $G/G_0 - \gamma$ curve from undrained triaxial experiments and literature on Oxford Clay



define the stiffness degradation curve. Three empirical methods of calculation were used to determine the parameter $\gamma_{0.7}$ as shown in Figure 5: a) Vucetic and Dobry (1991), (b) Vardanega and Bolton (2013) and c) Darendeli (2001). In addition, pressuremeter test data and triaxial testing (CKoU) were considered for derivation of $\gamma_{0.7}$. It is noted, however, that a smaller weighting was given to the pressuremeter tests as they are related to a different location with similar soil conditions and unknown soil stress history conditions. The characteristic at-rest earth pressure coefficient K_0 for the Oxford Clay was evaluated from triaxial testing and literature (Brosse et al., 2017) and ranged between 1.5 and 2.5.

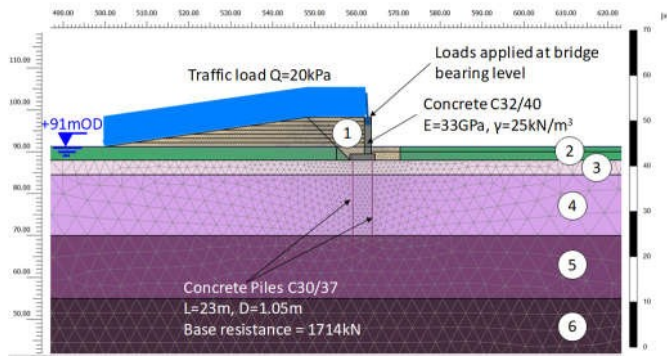
5. Analysis Results

5.1 K_a or K_0 earth pressure coefficient?

The mobilisation of active (K_a) or at-rest (K_0) static earth pressure behind the bridge abutment wall was one of the design challenges. To make an informed decision about the mobilisation of K_a or K_0 earth pressure distribution, 2D numerical analyses were conducted. A nonyielding inverted T-shape wall (founded on 23m piles) with a height of $H=10.2m$ (retained height $h=8.7m$) and heel length $b=3.4m$ was considered. The compacted dense granular backfill ($\phi=38^\circ$) behind the wall was applied in 7 steps in layers of 1m, an interface was defined with a maximum wall friction angle of $\delta = 27.6^\circ$. The numerical simulations were carried out using Plaxis 2D (Figure 6). The Mohr Coulomb (MC) and Hardening Small Strain Stiffness (HSS) material model used for the backfill (layer 1) and soil layers 2-6, respectively.

The soil lateral earth pressure distribution over the height of stem wall and the theoretical pressure distribution for active and at-rest state are shown in Figure 7. It should be noted that the K_0 and K_a coefficients are calculated using the Equation 8 proposed by Federico and Elia (2009) and Coulomb theory, respectively. According to the numerical model results, the abutment wall was displaced translationally $\sim 18.5mm$ and $23mm$ at bottom and top, respectively, to the active side and vertically $8.9mm$ at the toe and $\sim 6.8mm$ at the back of the heel). Also, the wall rotated clockwise by an angle $\theta \approx 0.02^\circ$.

Figure 6 Plaxis 2D finite element model



It is noted that the effect of soil-wall friction ($\delta = 21^\circ - 35^\circ$) on lateral earth pressure distribution was found to be negligible. Eurocode 7 (Appendix C.3) suggests that for non-cohesive dense soil, at-rest (K_0) conditions should be assumed if horizontal movement (u_h) normalised by the wall retained height (h) is less than a) 0.05% - 0.1% for translation mode and b) 0.1% - 0.2% for the top rotation mode. In practise, the designer can potentially assess the lateral wall deflection and rotation based on K_a lateral pressures acting on vertical virtual back plane and check against the movements to obtain an indication as to whether active or at-rest lateral earth pressure is mobilised based on the aforementioned criteria. However, other factors shall be considered whilst making this decision including the Category of the structure and this requires engineering judgment.

In this study, the ratio u_h/h is ranging from 0.19% – 0.23% for translation mode indicating that active earth pressure (K_a) is mobilised. On the other hand, the corresponding ratio due to wall rotation (assuming the wall is behaving as a rigid body) is 0.036% indicating that, according to both EC7 and Achmus (2017), at-rest (K_0) pressure is acting on the face of abutment wall. This means that an interim state between K_a and K_0 occurs along the stem wall height in line with field measurements of lateral pressures on retaining walls (see Coyle and Bartoskewitz 1970). Based on the numerical results, the earth pressures acting behind the abutment wall increase from active (K_a) at the top, to at-rest (K_0) at the bottom. However, K_0 pressures are mobilised along the vertical virtual back plane. A plausible explanation is that because of the existence of the heel length, a triangular soil wedge (BCD) occurs (see Figure 8) between the stem and the heel of T type cantilever retaining walls with short heel. Hence, the contact surface (or friction area) does not occur between the stem and the backfill (line BC in Figure 8). Correspondingly, due to the friction, less lateral earth pressure acts on upper (line AB) compared to the bottom part of the inverted T-shape wall. This behaviour agrees with the results presented by Achmus (2017). Interestingly, as shown in Figure 7, the earth pressure is higher than at-rest pressures at the bottom part of the wall (+92mOD). Below this level (i.e. structure's point of rotation) the relative movement between the stem wall and the backfill material, due to the rotation and the bending deformation of the stem wall indicates that the passive state occurs. It would be of particular interest if this could be confirmed by in-situ measurement of

Figure 7 Lateral earth pressure distribution over the wall height

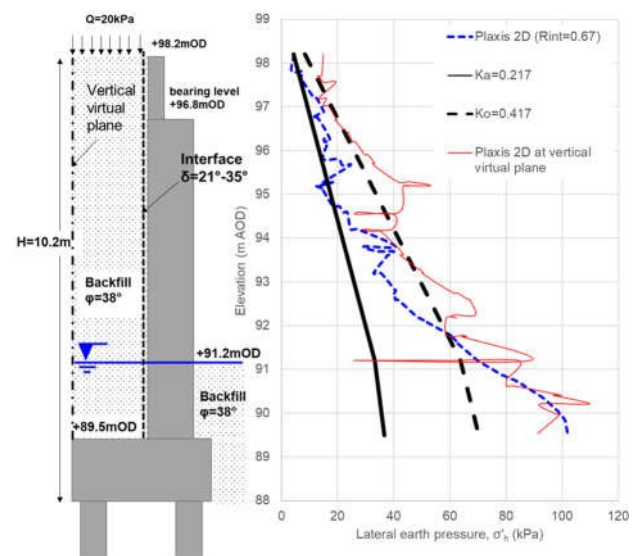
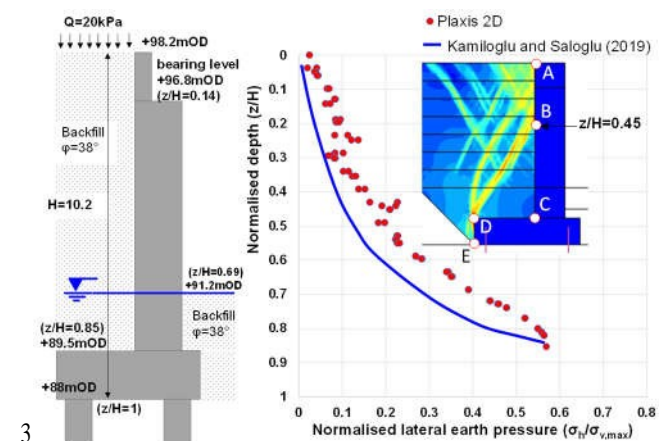


Figure 8 Normalised earth pressure distribution acting on the stem of the abutment wall



the lateral pressure as the study presented from Coyle and Bartoskewitz 1970, although this would be practically difficult. The normalised lateral earth pressure distribution ($\sigma_h/\sigma_{v,max}$) vs. normalized depth z/H acting on stem of the abutment wall above pile cap level is shown in Figure 8. It is seen that a scattered pressure distribution is obtained from the contact surfaces (line AB and DE). On the other hand, a smooth lateral earth pressure curve is observed from $z/H = 0.45 - 0.85$ where no strain fields occur (line BC). The normalized lateral earth pressure acting on the stem varies between 0.02 and 0.6. The above observations are in a good agreement with the results presented from Kamiloglu et al (2019).

5.2 Comparison of PIGLET, Repute and Plaxis 3D

The pile group shown in Figure 1 working under the general three-dimensional loading condition is assumed capped by a rigid pile cap in all the three pile group analysis software (i.e. PIGLET, Repute and Plaxis 3D) used. The loads applied at bottom of the pile cap level are presented in Table 1 and the

design methodology is described in Section 4. In all three software, the undrained shaft and bearing resistance of the piles were limited to the single pile capacity (calculated using the methodology outlined in Tomlinson & Woodward, 2007) for the specific soil conditions i.e. 77.3kPa and 1980kPa, respectively. The soil models used in the analysis software are shown in Table 2. In Plaxis 3D uniform loads were applied to generate the resolved forces and moments at the centre of the pile cap. The degree of anisotropy for Oxford clays ranges from 2-3 (Brosse et al., 2017). However, Plaxis 3D can only model isotropic soil behaviour. Therefore, the anisotropy $R=1$ used in PIGLET and Repute as well as at rest coefficient $K_0=1$ in Plaxis 3D was assumed throughout in all soil layers for each analysis.

Table 2 Soil models used in analysis software

Analysis Software	Soil model
Repute	Hyperbolic
Plaxis 3D	Hardening Small Strain Stiffness (HSS)
PIGLET	Linear increase (see Analysis 1 & 2)

In PIGLET analyses, the soil is modelled as a linear elastic material with a stiffness which varies linearly with depth. The influence of pile group size (O'Brien 2012) on the selection of the appropriate 'elastic' modulus is shown in Figure 9. Two analysis cases were examined in PIGLET:

- a) Analysis 1: selection of large strain stiffness (strain amplitude of 0.5%) at the pile head and intermediate strain (amplitude of 0.01%) stiffness at the pile toe level with a linear variation between these levels. The average $G/G_0-\gamma$ curve at the centre of the soil layers encountered along the pile length is used in Analysis 1 (Figure 9).
- b) Analysis 2: Elastic shear modulus (G) was taken as $300c_u$ (PIGLET manual).

Although the selected soil stiffness profile is different across all three software and the structural forces might be affected, the stiffness value is considered credible for design purposes.

It should be noted that Repute's hyperbolic model factors were compared against the vertical load test results as shown in Figure 3. In the same figure, the vertical load vs. settlement curve for a single pile for "Analysis 1" and "Analysis 2" are shown. The comparison shows a good agreement between the computed and the load-settlement behaviour derived from the pile test.

Figure 10 shows the comparison of the maximum (long term) pile cap settlement and lateral deflection. It is noted that the loading and consolidation stage were considered separately in Plaxis 3D as shown in Figure 10. The axial force (N), resultant shear force (Q) and bending moment (M) of corner pile No 7 are compared in Figure 11. The results indicate a general agreement between the three software. For the condition examined herein, the settlement predicted by the linear elastic analyses (i.e. PIGLET) is strongly affected by the selection of 'elastic' moduli. On the other hand, the effect of 'elastic'

Figure 9 Influence of pile-group size on the selection of the appropriate 'elastic' modulus.

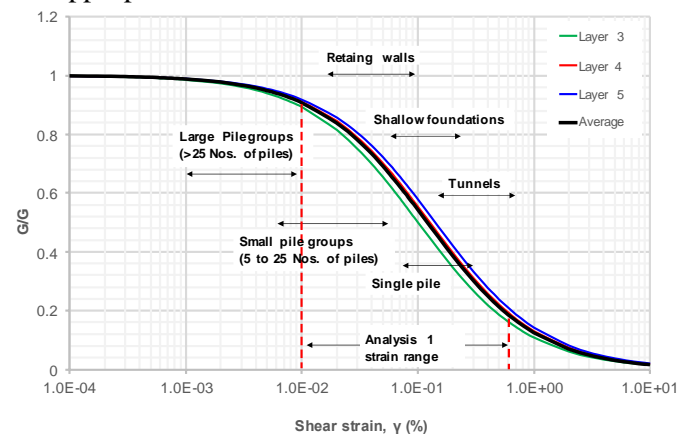


Figure 10 Pile cap movement (drained analysis) using Plaxis 3D, Repute and PIGLET

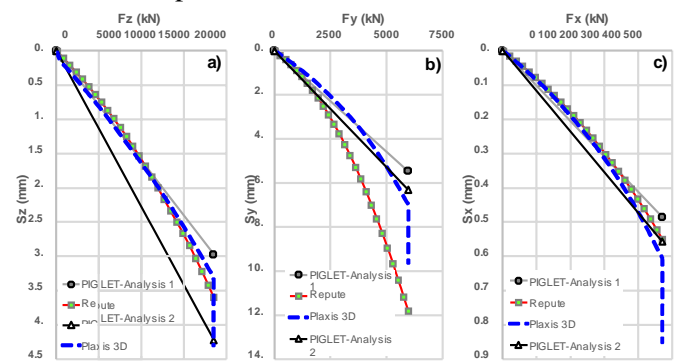
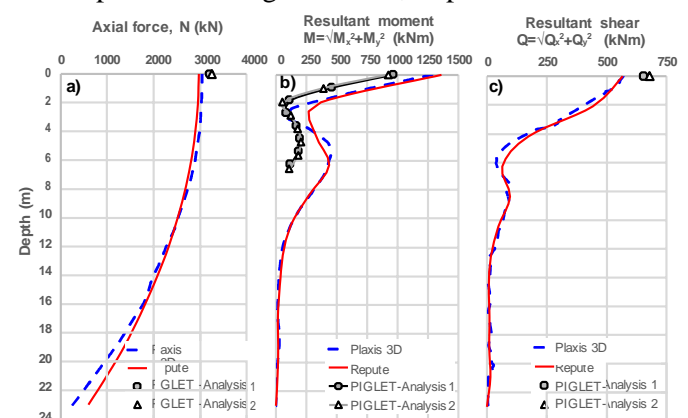


Figure 11 Structural forces (drained analysis) for the corner pile No.7 using Plaxis 3D, Repute and PIGLET



moduli on lateral movement is less pronounced. In comparison with non-linear analyses (i.e. Plaxis 3D and Repute), PIGLET results indicate: a) an over- or under-estimation of the settlement and under-prediction of the main lateral movement S_y (Figure 10a) and b) that under-predicts the horizontal movement independent of the selected shear modulus profile (Figure 10b). It should be noted that the lateral movement S_y predicted from Repute is higher compared to Plaxis 3D.

Figure 11 shows the structural pile reactions. The structural reactions of the corner pile No 7 calculated by Plaxis 3D are in

very good agreement with the pertinent results obtained from Repute. On the other hand, PIGLET over-estimates both the axial and shear force and under-predicts the resultant moment. It is worth noting that the pile cap stiffness is known to particularly affect the axial load in the corner pile in PIGLET, however the fully flexible cap option in PIGLET is only applicable for purely vertical loading conditions. Therefore, fully flexible pile cap option is not applicable in this study not only because the loading is applied in all three dimensions but also the pile cap is designed and behaved in a fully rigid manner to distribute load uniformly as the maximum span to thickness ratio of the cap is less than 5, (Gambhir 2011).

Following this assessment, it was determined that using REPUTE (hyperbolic model) was the most appropriate approach for the given structures and ground conditions, due to its versatility and ease of use. However, it will be interesting to verify the above predictions with field measurements, but at this stage no data are available as the railway overbridges are under construction.

6. Conclusions

The current study presents the bridge abutment pile group design methodology and key design challenges. More specifically, the following design challenges were investigated: a) the earth pressure distribution behind the stem of the abutment wall, b) the selection of an appropriate pile group design software package and c) linear vs. non-linear analysis. Based on the results presented in this study regarding a nonyielding inverted T-shape cantilever retaining wall subjected to high lateral loading, the following conclusions can be drawn:

1. The unconventional construction sequence (i.e. placement and locking of the deck prior to backfilling substructure) and the required structural rigidity to limit movements of the bridge bearings, indicate that the restrained movement of the structure is not sufficient to fully mobilise the active (K_a) earth pressures. The present study outlines a comprehensive methodology which can be followed in practice and can augment the database on lateral earth pressure distribution of cantilever retaining walls founded on piles.
2. Based on 2D numerical results and engineering judgement regarding the variability of the input parameters, the earth pressures acting behind the abutment wall decreased from active (K_a) at the top, to at-rest (K_0) at a certain level (point of rotation of the structure). Below this level the passive state occurs. The determination of the point of rotation of this structure is complex and hence the a priori prediction of the transition from active to passive state along the stem of the wall, is difficult without performing a numerical analysis. Notwithstanding the last remark, for practical use K_0 pressures combined with a vertical virtual back plane (which is advantageous as it leads to simpler geometry) can lead to satisfactory results and a reliable design where limiting movement is required.
3. The predicted movements and structural pile reactions using Repute and Plaxis 3D are in good agreement. In this

study, PIGLET under-predicts the lateral movement and bending moments but over-predicts the axial and shear forces. Although the selected soil stiffness profile is different across all three software and the structural forces might be affected, the stiffness value is considered credible in engineering practice.

4. The selection of a representative 'elastic' modulus profile is a key parameter to reliably perform a linear analysis and capture the pile group behaviour (i.e. PIGLET). In this study, linear analysis using PIGLET was not considered reliable for pile groups subjected to high lateral loads, even if the soil stiffness profile results in the same maximum pile group settlement among the software used. On the other hand, as is well known, non-linear analyses are capable of improved predictions, however good quality data on small to intermediate strain stiffness is required.

References

- El-Emam M (2011). Experimental and Numerical Study of At-Rest Lateral Earth Pressure of Overconsolidated Sand. *Advances in Civil Engineering*, Vol. 11, pp. 1-12.
- Achmus M (2017). Earth pressure acting on L-shaped walls. <https://www.igth.uni-hannover.de/winkelstuetzwaende.html?&L=1>.
- Brosse A *et al.* (2017) The shear stiffness characteristics of four Eocene-to-Jurassic UK stiff clays. *Géotechnique* 67(3): 242–259.
- Coyle HM and Bartoskewitz RE (1970). Field Measurements of Lateral Earth Pressures and Movements on Retaining Walls, Texas Transportation Institute, Texas A&M University.
- Federico A and Elia G (2009). At-rest earth pressure coefficient and Poisson's ratio in normally consolidated soils. *Proceedings of the 17th International Conference on Soil Mechanics and Geotechnical Engineering*, doi:10.3233/978-1-60750-031-5-7, pp. 7-10
- Kamiloğlu HA *et al.* (2019) Numerical analysis of active earth pressures on inverted T type and semi-gravity walls. *3rd International Conference on Advanced Engineering Technologies*, ICADET, Sept. 19-21.
- O'Brien A (2012) Pile-group design. In ICE Manual of Geotechnical Engineering Volume II (Burland J *et al.* (eds.)). ICE Publishing, London, UK, pp. 823-850.
- Pirello S and Poulos H (2013). Comparison of four pile group analysis programs. *International Symposium on Advances in Foundation Engineering*, ISAFE, Dec. 5-6.
- Vardanega PJ *et al.* (2019). The DINGO Database: June 2019, v1.0. University of Bristol, Bristol, UK, <https://doi.org/10.5523/bris.3r14qbdhv648b2p83gjqby2fl8>.
- Vardanega PJ and Bolton MD (2013) Stiffness of clays and silts: normalizing shear modulus and shear strain. *Journal of Geotechnical and Geoenvironmental Engineering* 139: 1575-1589.
- Tomlinson, M. and Woodward, J., (2007). Pile design and Construction Practice, 5th Edition, pp. 566.
- Gambhir, M.L., (2008). Design of Reinforced Concrete Structures.